A Domain Decomposition Technique for Computational Solid Dynamics*

John K. Prentice†
Michael M. Fikani†

Abstract. A domain decomposition technique has been developed for Eulerian solid dynamic continuum mechanics problems involving impact, penetration, shocks, and other high strain rate and large deformation phenomena. The technique is being implemented in TOLTEC, a multi-dimensional hydrocode.

1. Introduction. This paper discusses a domain decomposition methodology for modeling solid dynamic continuum mechanics problems involving impact, penetration, shocks, and other high strain rate and large deformation phenomena in solid materials. This methodology has been tested in two dimensions in an Eulerian computer code called DDHULL[2] and is currently being implemented in a new three dimensional Eulerian code called TOLTEC.

2. Governing Equations. The dynamics of isotropic elastic/plastic solid materials is governed by the equations for the conservation of mass, momentum, and energy:

$$\frac{\partial}{\partial t}\int_\Omega dV\rho = 0 \tag{1}$$

$$\frac{\partial}{\partial t}\int_\Omega dV\rho\vec{v} - \oint_{\partial\Omega} d\vec{A}\cdot\mathbf{T} = 0 \tag{2}$$

$$\frac{\partial}{\partial t}\int_\Omega dV\rho E - \oint_{\partial\Omega} d\vec{A}\cdot(\mathbf{T}\cdot\vec{v}) = 0 \tag{3}$$

coupled with the stress-displacement relation:

$$\frac{\partial \mathbf{S}}{\partial t} = 2\mu\frac{\partial\epsilon}{\partial t} \tag{4}$$

* This work performed at Amparo Corporation and funded in part by a Small Business Innovation Research Contract from the Armament Directorate at Eglin Air Force Base.

† Amparo Corporation, 3700 Rio Grande N.W., Suite 5, Albuquerque, New Mexico 87104-3042.

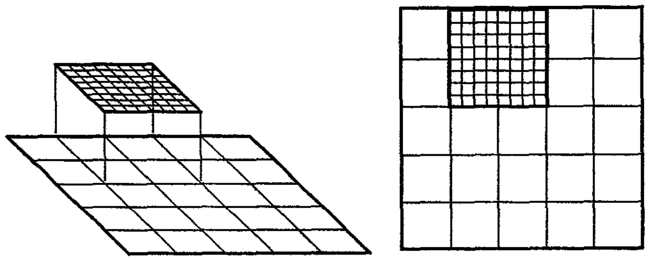

FIG. 1. *An example of a two dimensional composite mesh consisting of two overlapping sub-grids. The figure on the left shows the two sub-grids separately. The lines extending vertically from one sub-grid to the other show where the finely zoned sub-grid overlaps the coarsely zoned sub-grid. The figure on the right shows the finely zoned sub-grid embedded in the coarsely zoned sub-grid. The finely zoned sub-grid is defined to be the topmost sub-grid in the mesh hierarchy.*

and the pressure evolution equation:

$$\frac{\partial}{\partial t}\int_{\Omega} dV \frac{P}{\rho c^2} + \oint_{\partial\Omega} d\vec{A}\cdot\vec{v} = 0 \tag{5}$$

where t is time, ρ is material density, $\vec{v}$ is material velocity, $\mathbf{T}$ is the stress tensor, E is total specific energy, $\mathbf{S}$ is the deviatoric stress tensor, ϵ is the deviatoric strain tensor, μ is the shear modulus, P is hydrostatic pressure, and c is the speed of sound in the material. The integrals with respect to V are volume integrals over some spatial volume Ω and the integrals with respect to $\vec{A}$ are surface integrals over the boundary of Ω. The stress tensor is related to the deviatoric stress tensor and hydrostatic pressure by:

$$T_{ij} = S_{ij} - P\delta_{ij} \tag{6}$$

Plasticity is modeled by constraining the deviatoric stress tensor to lie on or below the yield surface for the material.

3. Domain Decomposition Methodology. These equations are solved in the spatial domain of interest by discretizing the domain with a composite grid consiting of one or more sub-grids. All hydrodynamic quantities are defined at cell centers in these sub-grids and the sub-grids are fixed in space. The cells in each sub-grid are right parallelpipeds and the grid lines are required to be parallel and continuous. In general, cells are choosen to be cubes in three dimensions or squares in two dimensions. The zoning choosen for each sub-grid is independent of the zoning in other sub-grids. This allows composite grids to be generated which have local mesh refinement in regions where good spatial resolution is required.

Sub-grids adjoin along common boundaries with other sub-grids to form the composite mesh. To accomodate more general mesh topologies, sub-grids are also allowed to overlap. In regions where sub-grids overlap, a grid hierarchy is defined and the equations are solved only in the topmost grid in this hierarchy. Figure 1 shows an example of a two dimensional composite mesh consisting of two overlapping subgrids.

In each sub-grid, equations (1) through (3) and equation (5) are solved using a second order accurate finite volume technique. The differential equation (4) is solved using a second order accurate finite difference technique. These equations are written

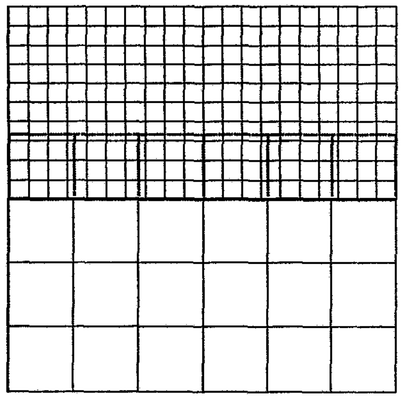

FIG. 2. *An example of phantom boundary cells from one sub-grid overlapping the interior of an adjoining sub-grid in two dimensions. The phantom boundary cells for the lower sub-grid are shown as dotted lines which project into the interior of the upper sub-grid.*

in a Lagrangian reference frame which moves with the material. This results in the sub-grids distorting slightly during each time step in order to conserve mass in each cell as required by equation (1). We are actually interested in a solution on fixed sub-grids, however. Hence at the end of each time step an advection calculation is performed which fluxes material across cell and sub-grid boundaries so that the distorted sub-grids can be mapped back onto the original sub-grids. The advection is performed using a van Leer[1] second order advection scheme in conjuction with a multi-material diffusion limiter which prevents material interfaces from diffusing during the advection phase.

The finite volume scheme uses initial cell centered values of the state variables to determine half time step advanced values on cell boundaries. These cell boundary values are then used to determine the cell centered values at the full time step. Generating the cell boundary values requires knowing the values of the state variables in the cells adjacent to the boundary of interest. At the exterior boundaries of each sub-grid, this is accomplished by defining a layer of phantom cells which are filled with state variables choosen to generate the correct boundary conditions. The boundary phantom cells are choosen to be the same size as the interior boundary cells. At points on a sub-grid boundary which do not adjoin another sub-grid, these phantom cells are filled by interpolating values from the interior of the sub-grid and adjusting the momentum components to give either a transmissive or reflective boundary condition. At points on a sub-grid boundary which do adjoin another sub-grid, the phantom cells of one sub-grid will overlap cells in the interior of one or more other sub-grids.

Figure 2 shows an example of the phantom boundary cells of one sub-grid overlapping the interior of another sub-grid. In these cases, the values of the state variables in the phantom cells are determined by a mass weighted interpolation of the state variables in the overlapped cells. Once the phantom cells are filled, the equations (1) through (5) are solved independently in each sub-grid to determine the state variables at the new time step. The advection calculation is then performed to map the distorted sub-grids back onto the original sub-grids. At boundaries between adjoining sub-grids, this advection will require fluxing material between the meshes. This is accomplished by filling the phantom cells of each sub-grid using the new time advanced state values. This information is then used by each sub-grid to independently calculate the amount of material to be advected across the boundaries. Only fluxes leaving a sub-grid are calculated using this method. Once these outgoing fluxes are determined for each sub-grid, material is advected between sub-grids. If a sub-grid boundary cell adjoins more than one boundary cell in another sub-grid, the outgoing flux is apportioned between these cells using a weighting scheme.

The advantage of this phantom cell method of imposing boundary conditions between sub-grids is that it is computationally inexpensive and eliminates the need for special treatment of the equations at the boundaries. In addition, since the phantom cells for a sub-grid have the same zoning as the interior cells, the impedance mismatch between finely zoned and coarsely zoned sub-grids is minimized. The main disadvantage is that adjoining sub-grids with different zoning may interpolate slightly different boundary conditions based upon the values in their phantom cells. To illustrate this problem, consider the common boundary between a finely zoned and a crudely zoned sub-grid. The phantom cells from the finely zoned mesh will project one row deep into the crudely zoned sub-grid. On the other hand, the phantom cells for the crudely zoned mesh will project several rows into the finely zoned sub-grid. The phantom cells for the crudely zoned mesh are thus sampling conditions deep in the interior of the finely zoned mesh and using these to determine boundary conditions. These boundary conditions will include information not available to the boundary cells in the finely zoned mesh and hence the boundary conditions that each sub-grid generates will be slightly different. The magnitude of the error introduced by this boundary condition mismatch is minimal, however, due to the small time step required by the explicit finite volume and difference schemes. Calculations have been performed of strong shocks crossing boundaries between sub-grids with zoning differing by a factor of ten without introducing significant pertubations at the boundary.

REFERENCES

[1] B. VAN LEER, *Towards the ultimate conservative difference scheme iv. a new approach to numerical convection*, Journal of Computational Physics, 23 (1977), pp. 276–299.

[2] M. WESTER AND J. PRENTICE, *Shock Compression of Condensed Matter - 1989*, North-Holland, 1990.